Video Article

Combined In Vivo Anatomical and Functional Tracing of Ventral Tegmental Area Glutamate Terminals in the Hippocampus

Amita Shrestha[1], Philip Adeniyi[1], Olalekan M. Ogundele[1]

[1]Department of Comparative Biomedical Sciences, Louisiana State University School of Veterinary Medicine

Correspondence to: Olalekan M. Ogundele at ogundele@lsu.edu

URL: https://www.jove.com/video/61282
DOI: doi:10.3791/61282

Keywords: circuit, optogenetics, AAV, firing rate, in vivo, recording

Date Published: 5/29/2020

Citation: Shrestha, A., Adeniyi, P., Ogundele, O.M. Combined In Vivo Anatomical and Functional Tracing of Ventral Tegmental Area Glutamate Terminals in the Hippocampus. *J. Vis. Exp.* (), e61282, doi:10.3791/61282 (2020).

Abstract

Optogenetic modulation of neuron sub-populations in the brain has allowed researchers to dissect neural circuits in vivo and ex vivo. This provides a premise for determining the role of neuron types within a neural circuit, and their significance in information encoding relative to learning. Likewise, the method can be used to test the physiological significance of two or more connected brain regions in awake and anesthetized animals. The current study demonstrates how VTA glutamate neurons modulate the firing rate of putative pyramidal neurons in the CA1 (hippocampus) of anesthetized mice. This protocol employs adeno-associated virus (AAV)-dependent labeling of VTA glutamate neurons for the tracing of VTA presynaptic glutamate terminals in the layers of the hippocampus. Expression of light-controlled opsin (channelrhodopsin; hChR2) and fluorescence protein (eYFP) harbored by the AAV vector permitted anterograde tracing of VTA glutamate terminals, and photostimulation of VTA glutamate neuron cell bodies (in the VTA). High-impedance acute silicon electrodes were positioned in the CA1 to detect multi-unit and single-unit responses to VTA photostimulation in vivo. The results of this study demonstrate layer-dependent distribution of presynaptic VTA glutamate terminals in the hippocampus (CA1, CA3, and DG). Also, the photostimulation of VTA glutamate neurons increased the firing and burst rate of putative CA1 pyramidal units in vivo.

Introduction

In the past decade, an array of genetic tools was developed to increase the specificity of neuron-type modulation, and the mapping of complex neural networks[1]. Notably, neurotropic viruses with an inherent ability to infect and replicate in neuronal cells have been deployed to express or ablate specific proteins in neuron sub-types. When harboring fluorescence proteins or genetically encoded synaptic activity indicators, transfected AAV vectors label and delineate neural networks across brain regions[2,3]. The choice of a promoter in the AAV construct directs the expression of the vector in neuron types with some level of specificity (**promoter-dependent** expression). However, through *Cre-lox* recombination, AAV constructs are deployed with greater specificity for ~~hypomorphic mutation,~~ neuron labeling[4,5], ~~and electrophysiology~~[6,7]. Of note, photoactivated microbial opsins and fluorescence proteins packaged in AAV vectors can be expressed in various neuron subtypes[8], and are ideal for imaging, neuron-type circuit tracing, and photomodulation[9,10].

AAVs constructs stereotactically injected into a brain region (or nucleus) drives the expression of the reporter protein in the soma, dendrite, and axons terminals. Neural expression of AAV harboring a reporter gene (eYFP) facilitates the labeling of neuron cell bodies and anatomical tracing of projections to and from other brain regions[11,12,13,14]. ~~In the same vein,~~ AAV-eYFP constructs carrying light-controlled opsin (e.g., hChR2), can be deployed as a tool for imaging[6,15] and simulation-based physiological tracing of neural projections to target brain areas in vivo[16]. Depending on the AAV serotype, the direction of neuron labeling may be anterograde or retrograde[11,12]. Previous studies have established that AAV5, ~~with a Calcium-Calmodulin-dependent kinase II alpha (CaMKIIα) promoter,~~ travels anterogradely in ~~CaMKIIα-positive~~ neurons[12]. ~~Owing to the described expression pattern~~, photostimulation of cell bodies expressing hChR2 produces presynaptic effects elsewhere in the brain (target)[17].

Here, AAV (serotype 5) with a CaMKIIα promoter was used to express eYFP (reporter) and hChR2 (opsin) in VTA glutamate neurons and axonal projections. Results from this study demonstrate the layer-dependent distribution of VTA-glutamate presynaptic terminals in the CA1, CA3, and DG hippocampal regions. Also, photostimulation of VTA glutamate neurons increased CA1 multi-unit and single-unit firing rates in vivowhen compared with baseline values. This protocol utilizes affordable tools and commercially available software that can increase the quality of data obtained from neural circuit tracing experiments.

Protocol

All experimental and animal handling procedures were approved by the Institutional Animal Care and Use Committee (IACUC) of the Louisiana State University School of Veterinary Medicine.

1. Experimental animal

1. Use 5–6 weeks old mice.

NOTE:To demonstrate this protocol, eYFP and hChR2 were expressed in VTA glutamate neurons using AAV5-mediated transfection under a CaMKIIα promoter (**Figure 1**). *Cre-lox* recombination can also be used for this step.

2. House 3–5 animals per cage under standard conditions of 12 h alternating light and dark cycle. Food and water should be provided ad libitum.

2. Craniotomy and animal preparation

NOTE:This section describes pre- and peri-operative procedures for mouse craniotomy. Use standard stereotactic apparatus and appropriate coordinates (Anteroposterior: AP, Mediolateral: ML, and Dorsoventral: DV). Refer to a mouse brain atlas to determine the coordinates for the brain region of interest.

1. Anesthetize mice by intraperitoneal ketamine (100 mg/kg)/xylazine (10 mg/kg) cocktail injection. Perform a toe pinch test to ensure the absence of sensation before the commencement of surgery.
   NOTE:Alternatively, Isoflurane anesthesia with an appropriate nose chamber can also be used for this step.
2. Gently fix the head of the animal on the stereotaxic apparatus.
   NOTE:It is important to handle animals with caution during this process. Also, check the breathing rate and other vitals before proceeding with surgery. Allow the animal to rest for ~7 min to reduce stress.
   1. Place a heating pad on the stereotaxic frame such that the body of the animal is lying on it. This will help maintain the body temperature and keep the animal warm though out the procedure. Retain the heating pad for postoperative care and recovery.
3. Use a clipper to remove hair over the scalp and clean the skin with an iodine solution.
   1. Apply topical lidocaine to block sensation on the scalp.
   2. Use a scalpel to make a midline scalp incision extending from the frontal to the occipital region.
   3. Clean the incision area with ~~saline~~, then expose the calvaria.
      NOTE:A small amount of 3% hydrogen peroxide solution can be applied to remove periosteum from the calvaria. This will increase the visibility of landmarks (bregma and lambda) and sutures.
   4. Using a mouse brain stereotactic atlas, determine AP and ML coordinates relative to the bregma.
   5. For VTA injection, position an ultrafine blunt-point needle syringe (e.g., Neuros syringe) at coordinates AP: -3.08 mm/ML: 0.5 mm relative to the bregma.
   6. Use a drilling tool to bore a 1 mm hole (craniotomy) in the skull at the marked AP/ML coordinate.
      NOTE:This step requires a significant level of caution. Minimal pressure should be applied while drilling to prevent the drill bit from crushing the brain tissue. In the current study, drill bit was 0.8 mm and drill speed was set to 15,000 rpm.
      CAUTION: If hydrogen peroxide was used in cleaning the incision or calvaria, ensure total removal of solution or allow complete dryness before drilling.

3. AAV cocktail injection

NOTE:This section describes the process for AAV injection into the VTA of adult C57BL/6 mice (23–27 g). The described method can be used for AAV injection into any brain region using standard stereotactic apparatus and appropriate coordinates.

1. Mount a syringe with ultrafine blunt-point needle (32 G; 5 µL capacity with 100 nL accuracy) on an injector. Fix the syringe holder on a micromanipulator.
   NOTE:For this procedure, a manual syringe holder, with 1.6 nL calibration, was used. An automated injector can also be used.
2. Fill the syringe with double distilled water to clean and test the flow of fluid.
3. Thaw aliquots of AAV (serotype 5) cocktail on ice. AAVs are best stored at -80 °C to maintain viral titer for good expression.
4. Fill the mounted syringe with 1,000 nL of AAV solution (10 mM in phosphate-buffered saline (PBS), pH 7.4). Dispense 10 nL of the AAV solution to confirm the flow of the liquid before lowering the needle into an injection site.
5. Use a micromanipulator to the syringe needle stereotactically into the desired depth (DV coordinate). After lowering the needle to the desired depth, allow the syringe to remain in place for 10 min before injection.
   NOTE:For this procedure, the needle was lowered into the VTA at a depth (DV) of 4.5 mm from the pial surface of the brain. For other brain areas, use the appropriate dorsoventral coordinate (refer to the mouse brain atlas).
6. Inject 600–800 nL of AAV into the VTA. Injection volume may be adjusted depending on the size of the target site.
   1. Deliver the AAV solution at the rate of 60 nL/min (3 min interval).
   2. To express eYFP and hChR2 in VTA glutamate neurons and projections, inject AAV-CaMKIIα-ChR2-eYFP.
      NOTE: *Cre-lox* recombination method can also be used depending on the goal of the experiment.
   3. Allow the needle to remain in place for 15 min after AAV injection. This will ~~allow for~~ diffusion and ~~reduce the~~ backflow.
7. Withdraw the syringe needle, and then suture the incision to close the wound.
8. ~~Apply topical~~ antibiotics and analgesia as a part of post-operative care. Place mice on warm padded platforms and monitor the animal until awake.
   NOTE:After 3 weeks of injection, AAV expression can be observed by fluorescence detection of reporter protein (eYFP) in mouse brain sections. Also, photostimulation experiments can be performed after 3 weeks (**Figure 2**).

4. Set up for in vivo neural recordings with optogenetics

NOTE:This section describes the steps for acute neural recording with the optogenetic tracing of a brain circuit (VTA glutamate neuron projection to the CA1). If necessary, check the system (amplifier and connections) for electrical noise and grounding issues before commencing this step. Performing this step in a Faraday cage can help eliminate electrical noise in the recording.

1. At 3 weeks after AAV injection, anesthetize mice by intraperitoneal urethane injection (0.2 mg/kg).
   CAUTION: Urethane is carcinogenic and must be handled cautiously while wearing protective gear. Also, administering urethane anesthesia at this concentration is non-survival ~~surgical procedures~~.
2. Affix the head of the animal on a stereotactic frame as described previously (step 2.2, **Figure 3A**). Perform a craniotomy to expose the dura (**Figure 3A**). Use a drilling tool (bit size: 0.8 mm, speed: 15,000 rpm) to remove part of the parietal bone (3 mm x 4 mm).
   1. The craniotomy should be about 3 mm x 4mm wide. Apply drops of artificial cerebrospinal fluid (aCSF) over this area to prevent dryness.
3. Under a dissection (digital) microscope, use a bent needle tip (27 G) to excise the exposed dura. Be careful not to pull apart the delicate pial covering and cortical tissues in this area.
4. Bore a hole in the ~~frontal~~ bone (bit size: 0.8 mm, speed: 10,000 rpm) to hold the ground screw (pan head Phillips screw; M0.6 x 2.0 mm).
5. Connect a ~~ground wire such as a~~ stainless-steel ground wire ~~(33 G) was used.~~
   NOTE:Other types of wires can also be used (**Figure 3b**).
6. For combined photostimulation (VTA) and neural recording (CA1), use a multi-rail stereotaxic apparatus fitted with ultra-fine (10 µm or 1 µm) micromanipulators. Mount the optical fiber and recording neural ~~electrode shank~~ on 10 µm-range and 1 µm-range micromanipulators, respectively.
   1. If necessary, use a head stage-probe adapter (**Figure 3c**).
      NOTE:In the current protocol, a 32-channel head stage was fitted with an adapter to hold a 4-channel recording electrode (**Figure 3d**). The stainless-steel ground wire was soldered to the ground connection port of the adapter.
7. At co-ordinates AP: -3.08 mm ML: 0.5 mm, lower the ~~2.5 mm~~ diameter ~~fiber~~ optic ~~cannula~~ into the VTA.
   1. Before lowering the ~~cannula~~, connect ~~the fiber optic cable (with stainless steel or ceramic ferrule) to a fiber coupled LED source.~~
      NOTE:Make sure light intensity and focus are set as desired. The choice of the LED light source should correspond to the opsins being targeted. Here, a 470 nm (blue light) LED driver was used for hChR2 photoactivation (**Figure 4a**).
   2. To synchronize the light pulse with the neural recording, connect the LED driver and recording controller digital **IN** port to a transistor-transistor logic (TTL) pulser (**Figure 4b**). This can be achieved using a BNC splitter.
      NOTE:The use of a TTL pulser provides the flexibility of digitally setting the desired pulse train frequency and duration. In the current protocol, 10 ms light pulses were triggered at 50 Hz[18]. For TTL control of the LED driver, switch the driver to “trigger”. In this mode, the light intensity can be regulated by turning the “knob”. Stimulation frequency can be adjusted to accommodate experimental variables, and could range from 1 to 100 Hz. For neural circuit tracing, a stimulation frequency of >~~40~~ Hz is recommended.
   3. Adjust the knob to determine the effective intensity that can generate a response without producing photoelectric artifacts. If necessary, reposition the optic fiber to eliminate artifacts[19].
      NOTE:The LED driver used for the current protocol produces light power of ~21.8 mW.

5. Neural recording

1. Use an acute neural probe with a 15–50 µm thick shank, measuring at least 5 mm in length.
   NOTE:Recording from deep brain structures will require neural probes with a longer shank. In the current study, a probe with 20 mm shank length was used.
2. Connect the pre-amplifier head stage to the recording controller via a serial peripheral interface (SPI) cable. Check LEDs color lighting on the recording controller ports. Green and yellow LEDs indicate proper voltage on the connected amplifier board. Red LED indicates a working software-head stage control (**Figure 5b**).

3. Using a micro-manipulator, position the electrode contact sites in the pyramidal cell layer of the CA1 (AP: -1.94mm, ML: +1.0mm, DV: +1.1 to 1.2mm).
NOTE: The optic fiber and electrode can be positioned in other desired brain regions for photostimulation and recording.

6. Amplifier and filter settings

1. Connect the recording controller amplifier system to a computer through a USB 3.0 port. Connect the head stage to the amplifier using the SPI cable. Launch the controller software. If not properly connected, the system will display a “device not found” message.
2. Click **Run** to view activity on the channels. Each waveform is plotted as the voltage (y-axis) versus time (x-axis). Depending on the region of interest, adjust the voltage and time scales to adjust the waveform display.
3. If only ~~a~~ few channels are active, disable unused channels to reduce file size on the storage disk.
4. Set the sampling rate and cut-off frequencies by editing bandwidth parameters on the acquisition software. For single-unit recording, set the upper and lower cutoff frequencies to 300 Hz and 5,000 Hz respectively. Change the amplifier sampling rate to 30 ~~KHz/s.~~
   NOTE:Choosing a high sampling rate will produce a larger file size.
5. Before recording, check the integrity of the electrode channels by measuring impedance at 1,000 Hz. This can be done by launching the function in the user interface (controller software). A working channel should have an impedance value that ranges from 0.1 to 5 MΩ.
6. If an audio output (speaker) is connected to **ANALOG OUT** port, adjust **gain** and **silencer** for optimum spike sound.
7. To display the TTL pulse train marker in the spike recording, enable the display for the **DIGITAL IN** marker. To record the pulse train time stamp, enable the **DIGITAL IN** channel display before the main experiment.
   NOTE:There is usually more than one “DIGITAL IN” channel (1 or 2). Ensure that the BNC cable from the TTL pulser is connected to the “DIGITAL IN” port that is selected for display in the recording controller software.
8. For real-time viewing of the spike waveform, open the spike scope window, and set threshold using the mouse click.

9. Inspect the noise level by monitoring the Root Mean Square (RMS in µV). For clean spike recording, it is preferred that the neural spike threshold is at least 5x RMS.
10. Once the setup is complete, select the file output format.
NOTE:Here, CA1 neural spike was recorded in .rhd format. Other file formats (.rhs and .dat) can also be selected to match the file formats permissible by the analysis software.

7. In vivo optogenetic recording and settings

1. Open the pulse control software (TTL) which displays various adjustable pulse parameters. Select the appropriate COM port on the software. Set pulse parameters by adjusting the **Train** and **Group** settings.
NOTE:The pulse condition should be determined by considering experimental variables and design.
2. On the amplifier controller software, click **Run** to detect neural spikes in the hippocampus or desired brain area. If necessary, adjust the electrode depth to detect viable and active neurons ~~(not more than 100 µm below the cell body layer)~~.
3. Once extracellular voltage activity is detected, observe baseline spikes for 15 min and monitor the vitals of the animal. Also, test the light pulse to detect responsive neurons within the CA1 or desired anatomical target region.
NOTE:Check for photoelectric artifacts and eliminate by adjusting light intensity or optic fiber position.
4. Record the baseline activity for ~10 min before triggering the light pulse at the desired frequency (**Figure 5a,b**). This will allow for comparison of firing or burst rates with and without illumination.
NOTE:In the current study, baseline activity was recorded for 10 min without illumination, followed by illumination at 50 Hz (**Movie 1**).

8. Analysis

1. Converter the .rhd file into Nex***5*** output format.
2. Process filename.Nex***5*** file in an offline sorter software to detect single unit raster trains and waveforms (**Figure 5a–b**).
    1. Select the desired channel from the drop-down window.
    NOTE:The continuously recorded spike data can be viewed on a separate window of the OFSS. The time scale can also be adjusted. If a tetrode is used, the OFSS can be set to sort the 4 channels as a tetrode.
    2. Set the voltage level for threshold crossing waveform extraction.
    CAUTION: Use a minimum of 5x RMS for proper spike detection.
    3. Detect waveforms, then perform spike sorting using valley-seeking (automatic) or K-means (semi-automatic) method. Where necessary, merge units that occupy similar regions of the 3D-Principal Component Analysis (PCA) space.
    4. Export sorted .Nex***5*** files for further analysis (**Figure 5c–d**).
    NOTE:Analysis outcomes for the interspike interval, firing rate, and burst rate can be exported into other analysis platforms.

9. Fluorescence detection of AAV expression

1. After the recording, euthanize the animal in an isoflurane chamber.
2. Perform transcardial perfusion with 10 mM PBS (~~60~~ mL), followed by 4% phosphate-buffered paraformaldehyde (PB-PFA, ~~60~~ mL).
3. Remove the whole brain intact and fix it in 4% PB-PFA for 48 h.
4. Transfer the fixed brain into 4% PB-PFA containing 30% sucrose for cryopreservation at 4 °C. After 72 h, section the brain in a cryostat and mount slices on a gelatin-coated slide.
NOTE:In the current protocol, slices containing the closed part of the hippocampus (rostral) ~~or VTA/open part of the hippocampus (caudal) were selected~~. Brain slices containing the VTA/hippocampus can also be processed for immunofluorescence detection of other proteins in the AAV-labeled neurons.

Representative Results

Anterograde tracing

AAV expression was verified by immunofluorescence imaging of reporter protein (eYFP) in the VTA of C57BL/6 mice 21 days post-injection (**Figure 2**). Successful anterograde labeling of presynaptic VTA glutamate projections in the hippocampus was also verified by eYFP detection in the layers of the DG, CA3, and CA1 (**Figure 6a–d**).

VTA glutamate projections to the hippocampus modulate CA1 activity

Photostimulation of VTA glutamate neurons increased the activity of putative pyramidal CA1 neurons. This is evident as an increase in spiking events during the light ON phase (**Movie 1**) when compared with the light OFF phase (**Figure 5a–b**). To support this outcome, statistical comparison of the CA1 network firing rates before (light OFF) and after (light ON) photostimulation revealed a significant increase for the post-stimulation period (**Figure 7a**; p = 0.0002). Subsequent analysis of the raster train to detect bursts (2–4 spikes in <16 ms) also demonstrates an increased burst rate for the CA1 putative pyramidal neurons after VTA glutamate photostimulation (**Figure 7b**; p = 0.0025). Statistical (Student's *t*-test) analysis was performed with standard software. Here, the baseline (light OFF) firing or burst rate was compared with light ON (photostimulation) values.

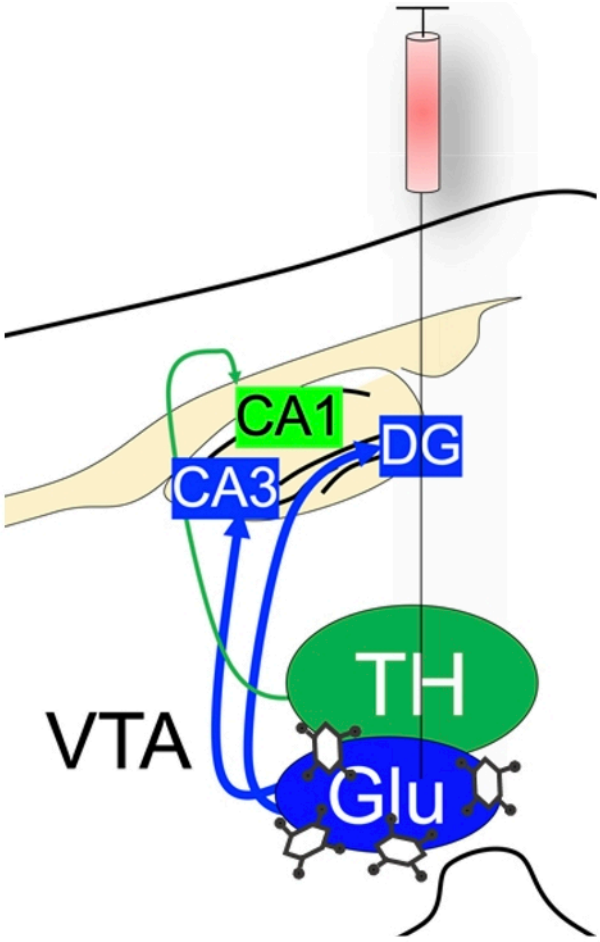

Figure 1: Schematic illustration of AAV-CaMKII-ChR2-eYFP injection into the VTA of C57BL/6 mouse.
~~This allowed for~~ anterograde labeling of VTA neurons and axonal projections to the hippocampus. Please click here to view a larger version of this figure.

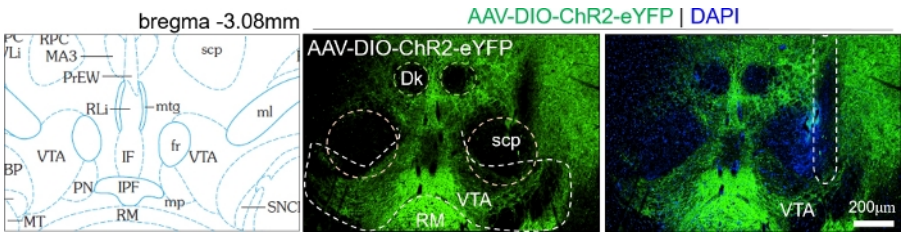

Figure 2: Fluorescence images showing AAV-CaMKII-ChR2-eYFP expression in the VTA, and optic fiber track.
Dk: nucleus of Darkschewitsch, scp: superior cerebellar peduncle, VTA: ventral tegmental area, and RM: retromamillary nucleus. Please click here to view a larger version of this figure.

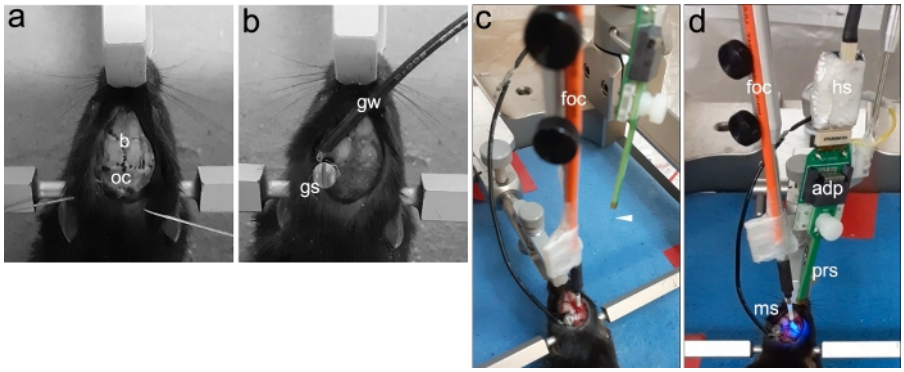

Figure 3: Demonstration of the craniotomy, electrode placement, and optic fiber placement.
(**A**) Midline incision exposing the cranium (b: bregma, oc: occipital bone). (**B**) Placement of the ground screw (gs) in the occipital bone and connected stainless steel ground wire (gw). (**C**) Stereotactic positioning of optic fiber cannula (foc: fiberoptic cable). (**D**) Stereotactic positioning of optic fiber cannula and neural probe shank (foc: fiberoptic cable, adp: adapter, ms: mating sleeve, prs: probe shank, hs: head stage). Please click here to view a larger version of this figure.

Figure 4: BNC split connection for combined light pulsing and amplifier (trigger) time stamps.
(**A**) Demonstration of LED light emission from the tip of an optic fiber cannula. (**B**) TTL pulse through a BNC split adapter to control LED and time stamp amplifier (ampl) recording. Please click here to view a larger version of this figure.

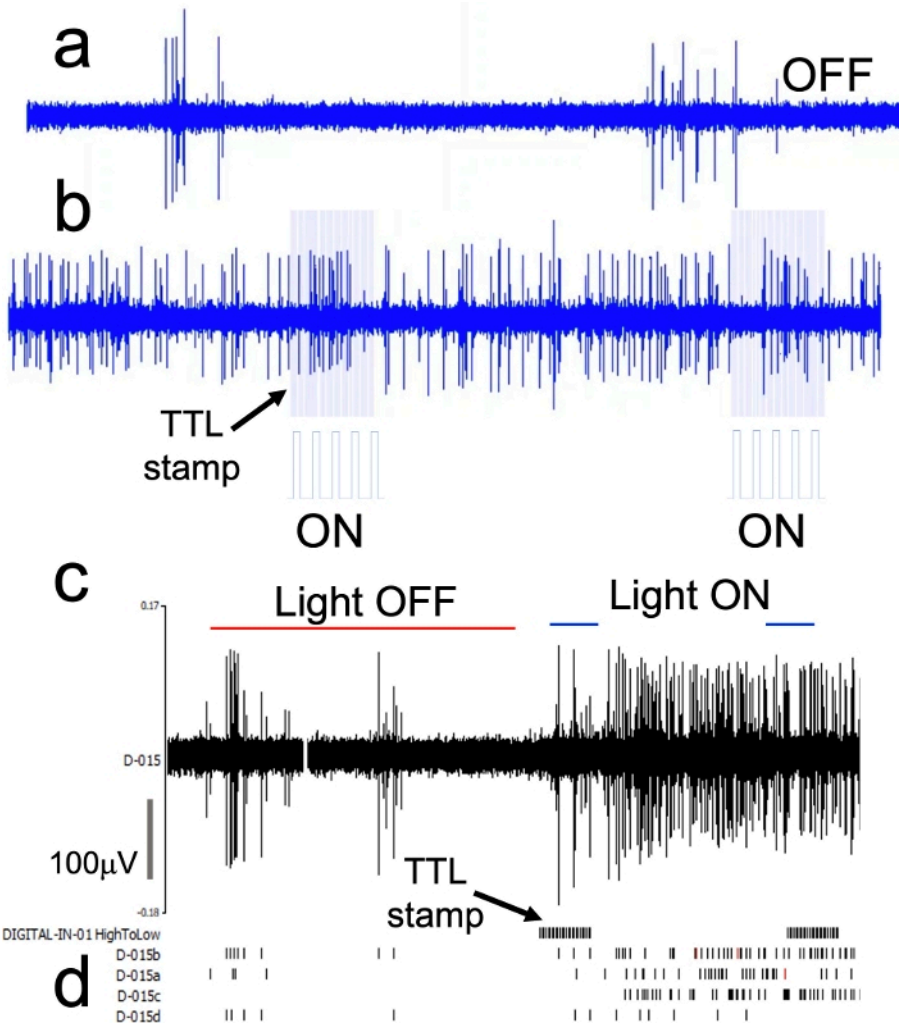

Figure 5: Continuously recorded spike train (raw data) with single unit detection.
(**A**) Screengrab of raw recording from the hippocampus of an anesthetized mouse. (**B**) TTL-driven photo illumination of the VTA in the raw recording. Light blue lines demonstrate the time stamps for Light ON (λ = 470nm) periods and frequency of stimulation. (**C–D**) Continuously recorded spike train and neuron units derived by spike sorting. Please click here to view a larger version of this figure.

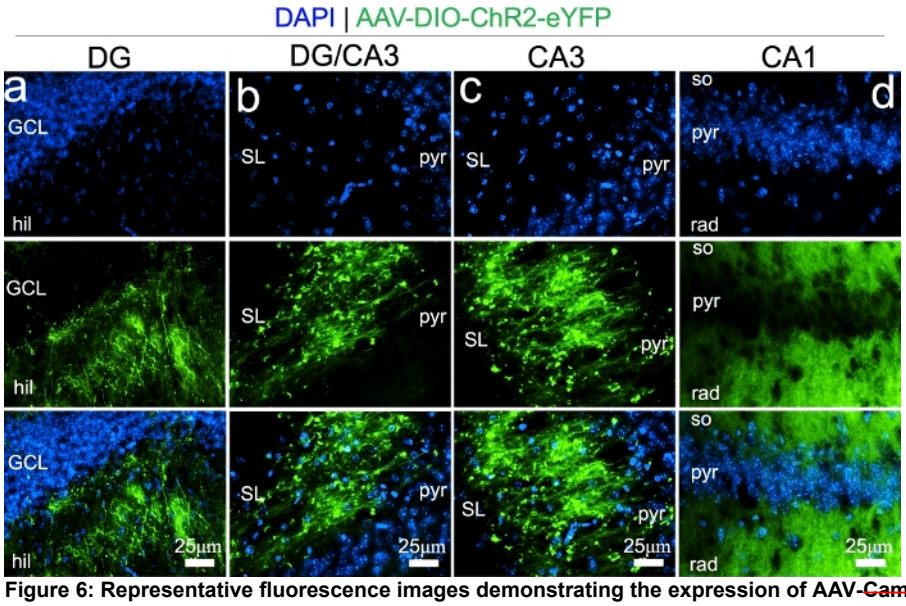

Figure 6: Representative fluorescence images demonstrating the expression of AAV-~~CamKII-~~ChR2-eYFP in the hippocampus. (**A**) DG (GCL: granular cell layer, hil: hilus). (**B**) Part of the CA3 close to the DG (SL: stratum lacunosum, pyr: pyramidal cell layer). (**C**) CA3 proper. (**D**) CA1 (so: stratum oriens, pyr: pyramidal cell layer, rad: stratum radiculata). Please click here to view a larger version of this figure.

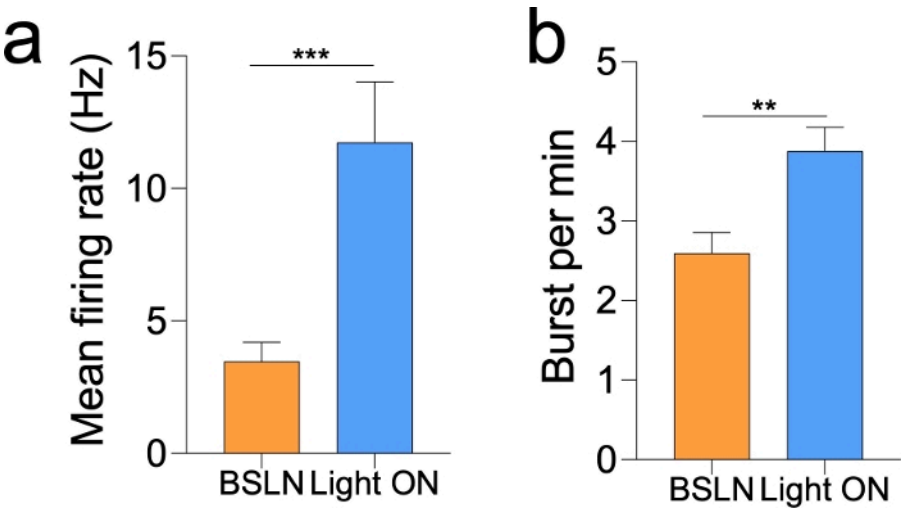

Figure 7: Statistical comparison of the firing rate before and after photostimulation. (**A**) Bar graph demonstrating an increased mean firing rate (Hz) for putative pyramidal neuron units in the CA1 (***p = 0.0002) after photo illumination. (**B**) Bar graph demonstrating an increased burst rate for putative CA1 neurons after photo illumination (**p = 0.0025). Error bar: standard error of mean. Please click here to view a larger version of this figure.

Movie 1: Screengrab recording of the amplifier controller and pulser software. The movie demonstrates baseline recording (light OFF) followed by photostimulation (light ON, λ = 470 nm) that is indicated with blue time stamps. Please click here to download this video.

Discussion

In the past decade, the design of AAV constructs has advanced significantly. As such, more neuron-specific promoters have been incorporated into an array of AAV serotypes for improved transfection specificity[14]. By combining genes for fluorescence proteins, transporters, receptors, and ion channels, libraries of AAV now exists for imaging, neuromodulation, and synaptic activity detection. In commercially available AAV-constructs, a combination of a genetically encoded fluorophore and ion channels (opsin) allows for a combined neuroanatomical and electrophysiological tracing of neural circuits[14,18,19]. Likewise, the selection of a promoter (or *cre-lox* recombination method) can permit the tracing of a neuron type-specific projections within a circuit. In the current study, this protocol was deployed for anatomical and electrophysiological assessment of VTA glutamate neural projections to the hippocampus (CA1 region).

VTA-Hippocampus neural circuit

The VTA is a part of the midbrain mesocorticolimbic pathway. VTA projections to brain areas involved in reward and aversion learning have been demonstrated extensively[20,21,22,23,24,25]. While the VTA contains dopamine, glutamate, and GABA neurons, the dopamine neuron population is anatomically dominant. A major function of the VTA in aversion and reward learning is attributed to a robust VTA dopamine projection to the

nucleus accumbens and dorsal raphe nucleus[22,24,25,26,27,28]. Although VTA dopamine and glutamate neurons project to the hippocampus, the function of the anatomically dominant VTA glutamate terminals is less studied compared with VTA dopamine terminals in the hippocampus[29,30].

The current protocol describes the use of an AAV5 construct harboring a fluorophore (eYFP) and light controlled opsin (hChR2) for the mapping of CaMKIIα-expressing VTA (glutamate) terminals in the hippocampus. Previous studies have established that VTA glutamate terminals are anatomically dominant in the hippocampus when compared with VTA dopamine terminals[29]. To demonstrate the VTA glutamate presynaptic terminals in the hippocampus, AAV(5)-CaMKIIα-hChR2-eYFP was transfected into VTA neuronal cell bodies. This labeled the cell bodies VTA glutamate neurons (within the VTA) and outlined VTA glutamate terminals within the layers of the hippocampus.

Although VTA glutamate presynaptic terminals innervate DG, CA3, and CA1, the results show layer-dependent variations for these three regions (**Figure 6a–d**). In the DG, AAV labeled VTA glutamate terminals are anatomically dominant in the hilus when compared with the granular cell layer. In the CA3, the VTA glutamate terminals are relatively abundant in the stratum lacunosum when compared with the pyramidal cell layer and stratum oriens. Whereas in the CA1, VTA glutamate terminals significantly innervate the dendritic layers (stratum oriens and radiatum) when compared with the pyramidal cell layer. The outcome of this study also demonstrates that photostimulation of the VTA glutamate neuronal cell bodies modulate the activity of the CA1 neural network in vivo. ~~This was seen as a~~ significant increase in ~~the~~ firing rate and burst rate during the photostimulation epoch (**Figure 7a–b**). This agrees with the anatomical distribution of VTA glutamate terminals in the dendritic layers of the CA1 (**Figure 6d**) where it may exert effects on hippocampal information encoding. In support of this observation, other studies have shown that the VTA is a primary determinant of hippocampal working memory encoding, and regulates the selection of information to be stored in long-term memory through the VTA-hippocampus loop[22,23,24,25,26,27,28,29,31,32,33,34].

Technical considerations

To successfully implement this protocol, the choice of AAV constructs should be determined based on the neuron type to be targeted. The researcher must identify a suitable promoter (a gene product) that is unique to the neuron type to be targeted. In the current study, a CaMKIIα promoter was used to drive the expression of eYFP and hChR2 in CaMKIIα expressing neurons. However, a *cre-lox* recombination method can also be used. In this case, a double floxed AAV5 can be expressed in the VTA of CaMKIIα-Cre mice. The promoter and *cre-lox* based expression methods are also applicable to other neuron types[35,36,37].

The system should be checked for electrical noise. This can be done by evaluating the RMS in spike scope during a trial recording session. If need be, the system and stereotactic apparatus should be housed in a Faraday cage, while the amplifier ground is connected to the cage. Electrode contact sites can be arranged linearly or ~~a~~ tetrode. The choice of probe design should be determined based on the objective of the experiment. A linear array detects neurons across multiple layers. Probes with various spacing (in microns) specifications are also commercially available. The shank length and distance between the probe contact sites should be considered during the recording procedure and for the analysis. When the setup is complete, the light pulse needs to be checked during a trial recording to eliminate photoelectric artifacts. This can also be optimized by adjusting the position of the electrode relative to optic fiber depth and location.

Limitations

Although CaMKIIα is expressed primarily in glutamate-releasing neurons, the protein is also present in some populations of dopamine neurons that co-release glutamate. Thus, using AAV5-CaMKIIα will mostly label glutamate neurons and some dopamine neurons that express CaMKIIα. LED driven photostimulation protocols are affordable and can be easily assembled. However, it is important to note that a laser-driven photostimulation protocol is more effective[38,39,40]. AAV solution injected into the same brain region for different animals yield varying expression thresholds. However, waiting for 3 weeks or more after the injection can reduce such variation by allowing optimum transfection. AAV solution injected into a brain region may also diffuse to surrounding brain areas. Observing the waiting period after the needle has been lowered, and in between bolus injections can reduce the diffusion of the AAV solution from the injection site.

In summary, this method can be used to trace neural circuits in the brains of rodents. Although the current protocol describes in vivo neural circuit tracing in anesthetized mice, the procedure can also be deployed for chronic recording in awake behaving mice.

Disclosures

The authors have nothing to disclose.

Acknowledgments

This work is funded by CBS Bridging Grant awarded to OOM. OOM, ~~PA~~, and AS designed the study and performed the experiments. AS and PA analyzed the results. OOM and PA prepared the manuscript.

References

1. Lo, L., Anderson, D. J. A Cre-dependent, anterograde transsynaptic viral tracer for mapping output pathways of genetically marked neurons. *Neuron.* **72** (6), 938-950, (2011).
2. Li, J., Liu, T., Dong, Y., Kondoh, K., Lu, Z. Trans-synaptic Neural Circuit-Tracing with Neurotropic Viruses. *Neuroscience bulletin.* 1-12, (2019).
3. Kuypers, H., Ugolini, G. Viruses as transneuronal tracers. *Trends in neurosciences.* **13** (2), 71-75, (1990).
4. Atasoy, D., Aponte, Y., Su, H. H., Sternson, S. M. A FLEX switch targets Channelrhodopsin-2 to multiple cell types for imaging and long-range circuit mapping. *Journal of Neuroscience.* **28** (28), 7025-7030, (2008).
5. Dragatsis, I., Zeitlin, S. A method for the generation of conditional gene repair mutations in mice. *Nucleic acids research.* **29** (3), e10-e10, (2001).

6. Gradinaru, V. et al. Molecular and cellular approaches for diversifying and extending optogenetics. *Cell.* **141** (1), 154-165, (2010).
7. Bernstein, J. G., Boyden, E. S. Optogenetic tools for analyzing the neural circuits of behavior. *Trends in cognitive sciences.* **15** (12), 592-600, (2011).
8. Tye, K. M., Deisseroth, K. Optogenetic investigation of neural circuits underlying brain disease in animal models. *Nature Reviews Neuroscience.* **13** (4), 251, (2012).
9. Mei, Y., Zhang, F. Molecular tools and approaches for optogenetics. *Biological Psychiatry.* **71** (12), 1033-1038, (2012).
10. Kohara, K. et al. Cell type–specific genetic and optogenetic tools reveal hippocampal CA2 circuits. *Nature Neuroscience.* **17** (2), 269, (2014).
11. Gombash, S. E. Adeno-Associated Viral Vector Delivery to the Enteric Nervous System: A Review. *Postdoc Journal.* **3** (8), 1-12, (2015).
12. Haggerty, D. L., Grecco, G. G., Reeves, K. C., Atwood, B. Adeno-Associated Viral Vectors in Neuroscience Research. *Molecular Therapy—Methods & Clinical Development.* **17** 69-82, (2020).
13. Montardy, Q. et al. Characterization of glutamatergic VTA neural population responses to aversive and rewarding conditioning in freely-moving mice. *Science Bulletin.* **64** (16), 1167-1178, (2019).
14. Yizhar, O., Fenno, L. E., Davidson, T. J., Mogri, M., Deisseroth, K. Optogenetics in neural systems. *Neuron.* **71** (1), 9-34, (2011).
15. Chamberlin, N. L., Du, B., de Lacalle, S., Saper, C. B. Recombinant adeno-associated virus vector: use for transgene expression and anterograde tract tracing in the CNS. *Brain Research.* **793** (1-2), 169-175, (1998).
16. Zingg, B. et al. AAV-mediated anterograde transsynaptic tagging: mapping corticocollicular input-defined neural pathways for defense behaviors. *Neuron.* **93** (1), 33-47, (2017).
17. Wang, C., Wang, C., Clark, K., Sferra, T. Recombinant AAV serotype 1 transduction efficiency and tropism in the murine brain. *Gene therapy.* **10** (17), 1528, (2003).
18. Ahlgrim, N. S., Manns, J. R. Optogenetic Stimulation of the Basolateral Amygdala Increased Theta-Modulated Gamma Oscillations in the Hippocampus. *Frontiers in Behavioral Neuroscience.* **13**, 87, (2019).
19. Buzsaki, G. et al. Tools for probing local circuits: high-density silicon probes combined with optogenetics. *Neuron.* **86** (1), 92-105, (2015).
20. Benardo, L. S., Prince, D. A. Dopamine action on hippocampal pyramidal cells. *Journal of Neuroscience.* **2** (4), 415-423, (1982).
21. Davidow, J. Y., Foerde, K., Galvan, A., Shohamy, D. An Upside to Reward Sensitivity: The Hippocampus Supports Enhanced Reinforcement Learning in Adolescence. *Neuron.* **92** (1), 93-99, (2016).
22. Hu, H. Reward and Aversion. *Annual Review of Neuroscience.* **39**, 297-324, (2016).
23. Kahn, I., Shohamy, D. Intrinsic connectivity between the hippocampus, nucleus accumbens, and ventral tegmental area in humans. *Hippocampus.* **23** (3), 187-192, (2013).
24. Lisman, J. E. Relating hippocampal circuitry to function: recall of memory sequences by reciprocal dentate-CA3 interactions. *Neuron.* **22** (2), 233-242, (1999).
25. Lisman, J. E., Grace, A. A. The hippocampal-VTA loop: controlling the entry of information into long-term memory. *Neuron.* **46** (5), 703-713, (2005).
26. Broussard, J. I. et al. Dopamine Regulates Aversive Contextual Learning and Associated In Vivo Synaptic Plasticity in the Hippocampus. *Cell Reports.* **14** (8), 1930-1939, (2016).
27. Hansen, N., Manahan-Vaughan, D. Dopamine D1/D5 receptors mediate informational saliency that promotes persistent hippocampal long-term plasticity. *Cerebral Cortex.* **24** (4), 845-858, (2014).
28. Salvetti, B., Morris, R. G., Wang, S. H. The role of rewarding and novel events in facilitating memory persistence in a separate spatial memory task. *Learning & Memory.* **21** (2), 61-72, (2014).
29. Ntamati, N. R., Luscher, C. VTA Projection Neurons Releasing GABA and Glutamate in the Dentate Gyrus. *eNeuro.* **3** (4), (2016).
30. Yoo, J. H. et al. Ventral tegmental area glutamate neurons co-release GABA and promote positive reinforcement. *Nature Communications.* **7**, 13697, (2016).
31. Funahashi, S. Working Memory in the Prefrontal Cortex. *Brain Sciences.* **7** (5), (2017).
32. Luo, A. H., Tahsili-Fahadan, P., Wise, R. A., Lupica, C. R., Aston-Jones, G. Linking context with reward: a functional circuit from hippocampal CA3 to ventral tegmental area. *Science.* **333** (6040), 353-357, (2011).
33. McNamara, C. G., Dupret, D. Two sources of dopamine for the hippocampus. *Trends in Neurosciences.* **40** (7), 383-384, (2017).
34. McNamara, C. G., Tejero-Cantero, A., Trouche, S., Campo-Urriza, N., Dupret, D. Dopaminergic neurons promote hippocampal reactivation and spatial memory persistence. *Nature Neuroscience.* **17** (12), 1658-1660, (2014).
35. Cardin, J. A. et al. Targeted optogenetic stimulation and recording of neurons in vivo using cell-type-specific expression of Channelrhodopsin-2. *Nature Protocols.* **5** (2), 247-254, (2010).
36. Mei, Y., Zhang, F. Molecular tools and approaches for optogenetics. *Biological Psychiatry.* **71** (12), 1033-1038, (2012).
37. Zingg, B. et al. AAV-Mediated Anterograde Transsynaptic Tagging: Mapping Corticocollicular Input-Defined Neural Pathways for Defense Behaviors. *Neuron.* **93** (1), 33-47, (2017).
38. Zhang, F. et al. The microbial opsin family of optogenetic tools. *Cell.* **147** (7), 1446-1457, (2011).
39. Aravanis, A. M. et al. An optical neural interface: in vivo control of rodent motor cortex with integrated fiberoptic and optogenetic technology. *Journal of Neural Engineering.* **4** (3), S143-156, (2007).
40. Oron, D., Papagiakoumou, E., Anselmi, F., Emiliani, V. Two-photon optogenetics. *Progress in Brain Research.* **196**, 119-143, (2012).

